International Journal of Naval Architecture and Ocean Engineering 13 (2021) 396–404

Contents lists available at ScienceDirect

International Journal of Naval Architecture and Ocean Engineering

journal homepage: http://www.journals.elsevier.com/international-journal-of-naval-architecture-and-ocean-engineering/

Uncertainty analysis of speed–power performance based on measured raw data in sea trials

Dae-Won Seo, Jungkeun Oh*

Department of Naval Architecure and Ocean Engineering, Kunsan National University, Kunsan, South Korea

ARTICLE INFO

Article history:
Received 15 September 2020
Received in revised form
30 March 2021
Accepted 6 April 2021

Keywords:
Monte Carlo simulation
ISO 15016
Uncertainty

ABSTRACT

It is important to verify that the contracted speed–power performance of a ship is satisfied in sea trials. International Organization for Standardization (ISO) has published the procedure for measuring and assessing ship speed during sea trials. The results obtained from actual sea conditions inevitably include various uncertainty factors. In this study, double run tests were performed on one container ship to analyze the uncertainty of sea trial on three maximum continuous rating conditions. The uncertainty factors and scale of uncertainty were examined based on the measured raw data during sea trial. The results indicate that the expanded uncertainty for ideal power performance is approximately ±1.4% at 95% confidence level (coverage factor k = 2) and most of the uncertainty factors were because of the shaft power measurement system.

1. Introduction

Typically, after a ship is built in a shipyard, various tests are conducted until the ship is delivered to the owner. The tests are broadly divided into on board tests and sea trials. The purpose of these tests is to provide a confirmation to the ship owner and classification society that the ship has been constructed in accordance with the contract and regulations. The installed equipment is inspected and sea trials are performed to confirm the performance of the ship with respect to speed and power in actual sea conditions.

The speed and power performance of the ship measured in sea trials can vary based on environmental conditions such as wind, wave, and water temperature. Hence, it is necessary to correct the speed and power performance measured in actual sea conditions to the values in calm sea conditions without disturbance. Specifically, ISO has published guidelines for assessing speed and power performance via the analysis of sea trial data.

The uncertainty in speed and power performance is determined by the level of accuracy of the measured values of shaft power and environmental disturbances. To reduce the uncertainty in speed and power performance measured in actual sea conditions, instruments with low error should be utilized. Furthermore, the measurements should be conducted in an ideal environmental condition such as still water. However, it is not always easy to conduct measurements under ideal environmental conditions. Therefore, all results of speed and power performance include uncertainty due to the measuring system and environmental correction (Insel, 2008). As the total uncertainty increases, the reliability of the speed and power performance decreases.

The International Towing Tank Conference (ITTC) proposed uncertainty guidelines for Computational Fluid Dynamics (CFD) analysis and various fluid dynamic experiments such as experiments involving resistance, self-propulsion, and propeller open water tests (ITTC, 2002; ITTC, 2005). Park et al. (2003, 2015) and Han et al. (2017) performed uncertainty analysis on resistance and self-propulsion experiments. Park et al. (2012), Seo et al. (2016), and Kinaci et al. (2018) conducted uncertainty studies on the numerical calculation of ship motion and resistance and propulsion analysis. Thus, most studies on guidance and uncertainty analysis primarily focus on laboratory-level experiments.

However, to date, a standardized uncertainty procedure for shaft power in sea trials has not been reported. Insel (2008) analyzed the uncertainty in shaft power performance based on a series of 12 vessels. Coraddu et al. (2014), Aldous (2015) and Tillig et al. (2018) investigated the uncertainty in the measured shaft power based on big data of port to port measured through the installation of a monitoring system.

In this study, uncertainty analysis was conducted to investigate

* Corresponding author.
E-mail address: jkoh@kunsan.ac.kr (J. Oh).
Peer review under responsibility of The Society of Naval Architects of Korea.

https://doi.org/10.1016/j.ijnaoe.2021.04.001

Table 1
Comparison of strengths and weaknesses of uncertainty analysis methods.

	Strength	Weakness
GUM	- Most widely used in the model experiment field - Law of propagation uncertainty - Input uncertainty based on type-A and type-B - Mathematical model (Tayler series method)	- Linear mathematical model - Gaussian Distribution (input data)
Monte Carlo simulations	- Most widely used in the risk assessment field - Law of propagation of distribution - Input uncertainty based on probability distribution - Monte Carlo simulation (iterative calculation) - Not restricted to distribution of input uncertainty	- Iterative calculation<
Analytical method	- No approximation - Highest reliability	- Simplest linear mathematical model

Table 2
Type-A and type-B uncertainties.

	Type-A	Type-B
Expression	$u_i^2(\bar{q})$	u_j^2
Measurement	Repeated observation	Previous data and Manufacturer's specification certificates

uncertainty factors and sensitivity based on the measured raw data in sea trials.

2. Method of the uncertainty analysis

Methods for uncertainty analysis can be classified into three categories, as shown in Table 1(ISO 19030, 2016). The first method, the ISO Guide to the expression of Uncertainty in Measurement (GUM) method, uses the uncertainty propagation law proposed in ISO JCGM 100(ISO, 2008a). The Taylor series is used to calculate the sensitivity coefficient, uncertainty contribution, and degree of freedom. This method has been widely used in the field of model experiment because it involves simple calculations. However, this method can only be used if the formula is linear and if the distribution of input data follows a Gaussian distribution.

To apply this method, standard uncertainties of type-A and type-B are calculated for each input variable, as shown in Table 2. The type-A standard uncertainty implies that an uncertainty component originating from randomness during the measurement can be evaluated via repeated measurements. Conversely, the type-B standard uncertainty is defined as the uncertainty of all components except their type-A standard uncertainty. It can be estimated from previous measurements, experimental data, general knowledge, and instrument specification. Based on the estimated type-A and type-B standard uncertainties, the total standard uncertainty of each input variable is calculated via Eq. (1) as follows:

$$u(y) = \sqrt{\sum_{i=1}^{N} u_i^2(\bar{q}) + \sum_{j=1}^{N} u_j^2} \tag{1}$$

In cases where the formula is defined as a function of several variables, the combined standard uncertainty is calculated using Eq. (2) as follows:

$$u_c(y) = \sqrt{\sum_{i=1}^{N} \left(\frac{\partial f}{\partial x_i}\right)^2 u^2(x_i) + 2\sum_{i=1}^{N-1}\sum_{j=i+1}^{N} \frac{\partial f}{\partial x_i}\frac{\partial f}{\partial x_j} u(x_i, x_j)} \tag{2}$$

where, the first term on the right denotes the uncertainty contribution for each input variable and the second term denotes the correlation between input variables, which can be assumed as zero because there is no correlation between input variables.

The expanded uncertainty (U) is a form of the product of coverage factor (k) and the combined standard uncertainty ($u_c(y)$), as shown in Eq. (3). The coverage factor is approximately 2 assuming a normal distribution in the 95% confidence interval.

$$U = ku_c(y) \tag{3}$$

The second method for uncertainty analysis involves the application of Monte Carlo simulations (ISO, 2008b). Contrary to the method involving the uncertainty propagation law, this method has no limitation on the formula. Hence, it is applicable even if the distribution of input variables does not correspond to Gaussian distribution. The key point in Monte Carlo simulation involves predicting the results through repeated simulations based on the concept that more accurate estimation results can be obtained by increasing the number of samples.

Monte Carlo simulation method has been systematized with the development of higher computational abilities of modern computers. Thus, it is used as a modeling method to reproduce actual situations. Specifically, this method is used in various fields because there are no limitations on the probability distribution of input variable and formula. In ship and offshore applications, Monte Carlo simulation has been used for evaluating the reliability of ship damage (Brown and Chen, 2002; Sun et al., 2017), cost optimization of construction (Para-Gonzalesz et al., 2018), and performance analysis of propulsion (Hang et al., 2018).

The implementation process of the Monte Carlo simulation is shown in Fig. 1. This process can be divided into the following four stages.

(1) defining the mathematical formula;
(2) assigning a probability distribution function to each input variable;
(3) performing the iterative calculation; and
(4) analysis of results.

3. Uncertainty analysis on the measured shaft power

In general, it is challenging to directly measure the power of the main engine in a sea trial. There is a direct method and indirect method to measure the shaft power of a ship. First, the shaft stress can be directly measured by installing a strain gauge or an optical

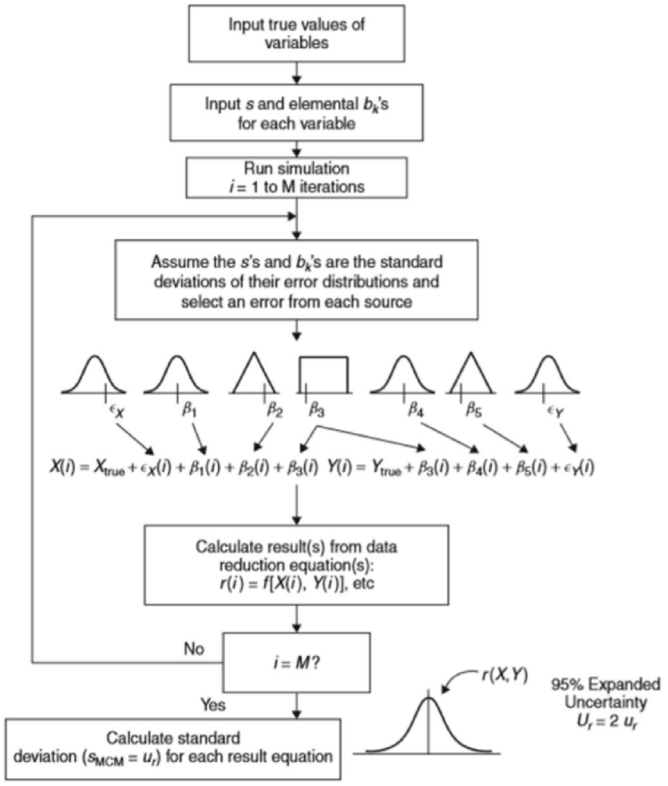

Fig. 1. Schematic of Monte Carlo method for uncertainty propagation (Coleman and Steele, 2009).

device on the shaft. Second, the combustion pressure of an engine can be converted into shaft power. However, this method exhibits inaccuracies due to fluctuations owing to periodic explosions in the engine. Hence, a direct method using a strain gauge is mainly used to measure the shaft power in actual sea conditions. In the case of the direct method using a strain gauge, a difference of voltage due to the torsional deformation of shaft is detected via the strain gauge, and the voltage is amplified as shown in Fig. 2.

The strain gauge signal measured on the shaft is wirelessly transmitted to the pickup unit via an installed antenna wire on the shaft. The output signal is converted into shaft power via the processing unit.

Hence, there are various uncertainty factors, such as uncertainty in the process of signal transmission, uncertainty in power conversion, and uncertainty due to errors in gauge installation.

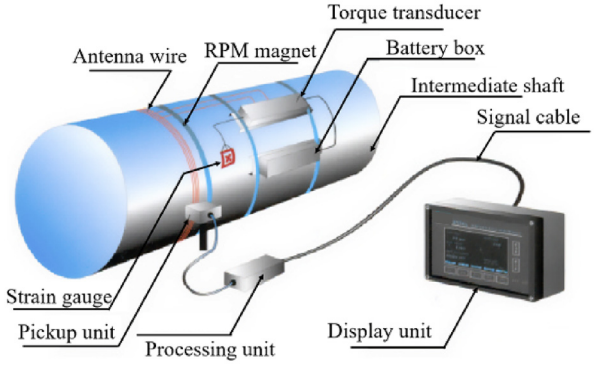

Fig. 2. Shaft power measurement system in sea trials.

The measured shaft torque (Q_{ms}) and shaft speed (η_{ms}) are converted to delivered power (P_{Dms}) using Eq. (4) as follows:

$$P_{Dms} = Q_{ms} \times \eta_{ms} \times \frac{2\pi}{60} \tag{4}$$

The uncertainties that may occur while measuring shaft power are divided into type-A and type-B. Although there are various instruments for measuring shaft power, existing systems frequently use strain gauges to measure the torque, which is converted into power with respect to the relationship with the shaft speed. This study used the Kyma Shaft Power Meter. The accuracy of the equipment yields useful data when evaluating type-B uncertainty.

The type-B uncertainty $u_c(Q_{ms})$ factors of the shaft power include the uncertainty of the strain gauge $u(gauge)$, the calibration uncertainty $u(\varepsilon)$, the uncertainty that occurs when installing sensors $u(\alpha)$, and torque calculation uncertainty $u(Q)$. Each of these can be subdivided as shown in Fig. 3, and the type-B uncertainty $u_c(Q_{ms})$ for measuring shaft torque is calculated using Eq. (5).

$$u_c(Q_{ms}) = \sqrt{u^2(gauge) + u^2(\varepsilon) + u^2(\alpha) + u^2(Q)} \tag{5}$$

As a result of examining the specifications of the shaft power measurement system and previous study(Seo et al., 2019), the total uncertainty including uncertainties that can occur when installing and calibrating the gauge and sensor is 0.316% and 0.370% respectively. A strain gauge of 350 Ω is used in the shaft torque measurement system in general. After adding the combined uncertainty(1.211%) from calculating the shaft torque (shear modulus standard uncertainty, shaft diameter standard uncertainty, relative displacement standard uncertainty), the total combined uncertainty of the shaft power measurement system $u_c(Q_{ms})$ becomes 1.385%. And the uncertainty of rotational speed measurement system $u_c(N_{ms})$ is approximately 0.06%, as shown in Table 3.

Therefore, the total combined uncertainty of the shaft power

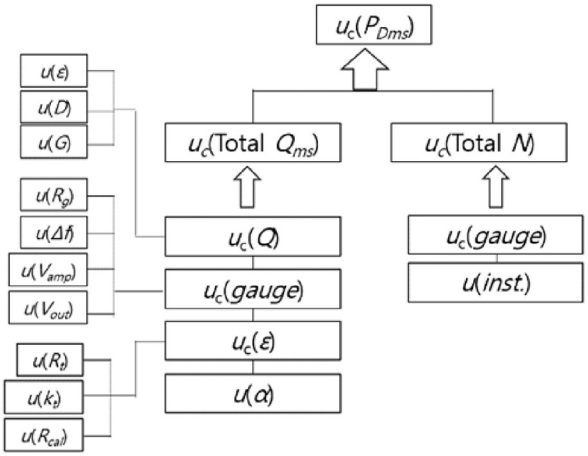

Fig. 3. Uncertainty sources in measurement of shaft power (Seo et al., 2019). *uc(PDms):* Uncertainty of the power measurement system, *uc(*Total *Qms):* Combined uncertainty of the total torque, *uc(Total N):* Combined uncertainty of the total shaft speed, *uc(Q):* Uncertainty due to recalculation of the torque, *uc(gauge)*: Uncertainty due to the gauge of shaft speed, *u(inst.)*: Uncertainty due to installation on a shaft, *uc(ε)*: Uncertainty due to calibration. *u(α):* Uncertainty due to strain gauge installation, *u(ε)*: Uncertainty of the relative strain of the gauge, *u(D):* Uncertainty of the diameter, *u(G):* Uncertainty of the shear module, *u(Rg)*: Uncertainty of the strain gauge bridge. *u(Δf)*: Uncertainty of the transmitter and receiver, *u(Vamp)*: Uncertainty of the amplifier plug-in module, *u(Vout)*: Uncertainty of the digital voltage meter, *u(Rt)*: Uncertainty of the strain gauge effective resistance, *u(kt)*: Uncertainty of the gauge factor at 75&ring. *u(Rcal)*: Uncertainty of the resistance of standard resistor.

Table 3
Uncertainty of type-B on the shaft power measurement system.

$u_c(P_{ms})$: 1.386	u_c(Total Q_{ms}): 1.385	$u_c(Q)$: *1.211*	$u_c(\varepsilon)$: 0.370 $u(D)$: 0.029 $u(G)$: 1.15
		$u_c(gauge)$: 0.462	$u(R_g)$: 0.231 $u(\Delta f)$: 0.294 $u(V_{amp})$: 0.183 $u(V_{out})$: 0.200
		$u_c(\varepsilon)$: 0.370	$u(R_t)$: 0.231 u(k_t): 0.289 $u(R_{cal})$: 0.00005
		$u_c(\alpha)$: 0.316	
	$u_c(N)$: *0.06*		

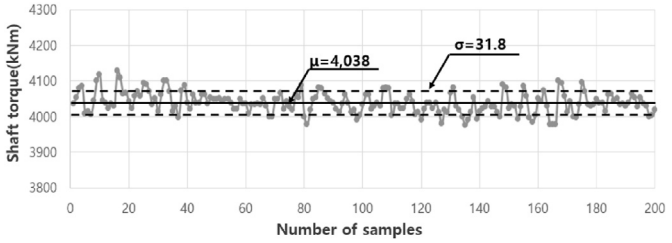

Fig. 4. Raw data of measured shaft torque (MCR 70%).

$u_c(P_{Dms})$ calculated using Eq. (6) becomes 1.386%.

$$u_c(P_{Dms}) = \sqrt{u_c^2(Q_{ms}) + u_c^2(N_{ms})} = \sqrt{1.385^2 + 0.06^2} = 1.386\% \quad (6)$$

The target ship for sea trial is 13,000TEU container ship with LBP of 350 m and B of 48.4 m. The sea trial was carried out in the Indian Ocean, 300 nautical miles east of Sri Lanka.

Fig. 4 and Fig. 5 show measured shaft torque and shaft speed measured every 3 s for 10 min under the condition of MCR 70%-1st run. The average values of the measured shaft torque and rotational shaft speed were 4038kNm and 75rpm, and the standard deviations were 31.8kN and 0.09rpm, respectively. The cause of the standard deviation of shaft torque and shaft speed is the influence of uncertainty in the measurement system and disturbances in the marine environment.

The probability distribution of the measured raw data is investigated to apply Monte Carlo simulation. Figs. 6 and 7 show the characteristics of the frequency and probability on the measured shaft torque and shaft speed at Maximum Continuous Rating (MCR) 70%-1st run condition. The Crystal ball software program is used to examine the probability distribution of raw data through the Anderson–Darling method. Hence, the probability distribution of the measured shaft torque and shaft speed has a Gaussian distribution.

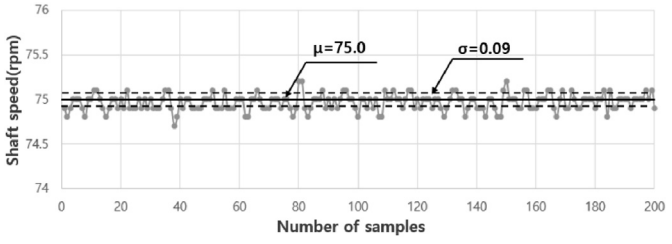

Fig. 5. Raw data of measured shaft speed (MCR 70%).

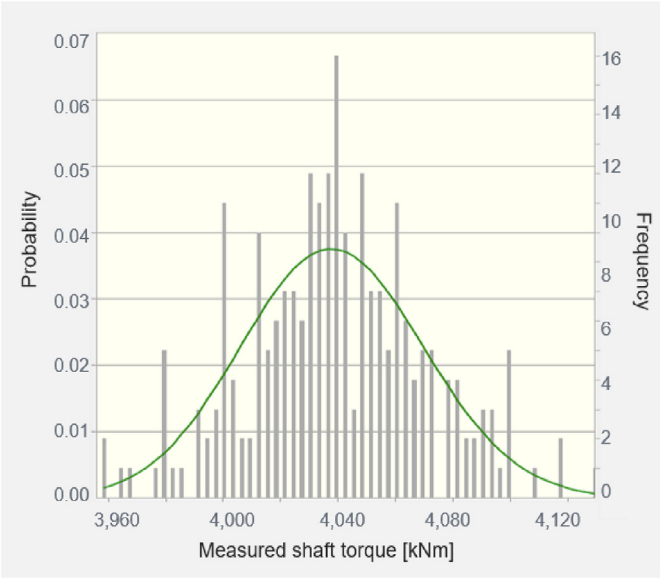

Fig. 6. Probability distribution on the measured shaft torque (MCR 70%).

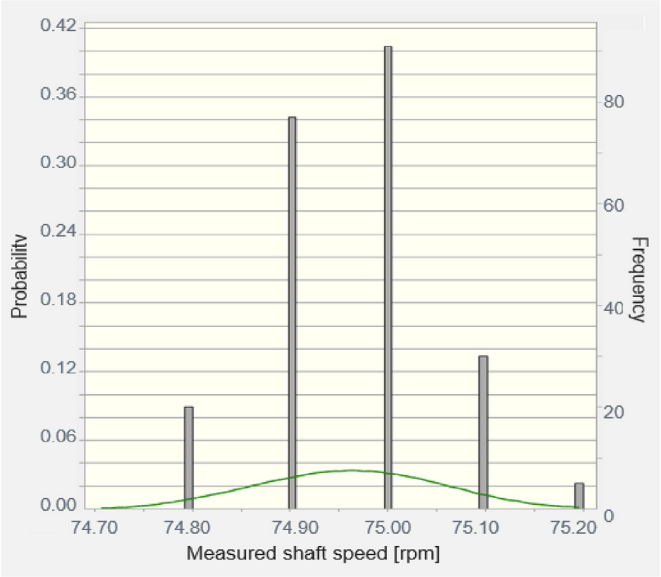

Fig. 7. Probability distribution on the measured shaft speed (MCR 70%).

Based on the type-A uncertainty of the measured data in sea trials and type-B uncertainty of shaft power measurement system, Monte Carlo simulation is performed 50,000 times to estimate the uncertainty of the shaft power measurement system via Eq. (4). Table 4 summarizes the results of the uncertainty analysis of the measured shaft power.

The expanded uncertainty of the measured shaft power is ±375 kW, which is approximately ±1.62% in the 95% confidence interval of coverage factor (k) of 2 under MCR 50%. The expanded uncertainty of the measured shaft power at MCR 70% and 80% is estimated as ±1.45% and ±1.73% respectively.

The rankings of each inputted variables were assessed using a sensitivity analysis with Crystal Ball software. Contribution to variance was calculated by squaring the rank correlation coefficient values and normalizing them to 100%. Contribution to variance showed sensitivities as values that range from 0 to 100% and

Table 4
Results of uncertainty analysis on measured shaft power (P_{Dms}).

	U (95%, k = 2) (kW)	U (95%, k = 2) (%)
50%	±375	±1.62
70%	±451	±1.45
80%	±606	±1.73

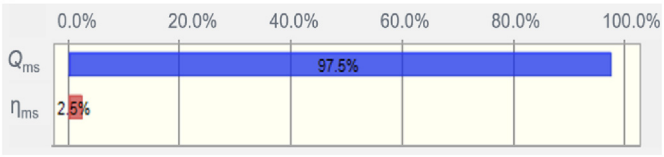

Fig. 8. Contribution to variance chart of uncertainty factor on the predicted shaft power (MCR 70%).

indicated relative importance by showing the percentage of the variance of the predicted variable contributed by each model input variable(Liang and Hu, 2017).

The contribution to variance on the measured shaft power are shown in Fig. 8 at the MCR 70% condition. Most of the uncertainty is attributed to shaft torque measurement (Q_{ms}), which accounts to approximately 98%. This implies that the large uncertainty factor in the shaft power measurement is due to the shaft torque measurement (Q_{ms}) as opposed to the shaft speed measurement (η_{ms}). Hence, it is necessary to measure the shaft torque more precisely to reduce the uncertainty in the shaft power during sea trials.

4. Uncertainty analysis on correction due to environmental effects

4.1. Measured average environmental data in sea trials

The average values of the characteristics for wind and wave are shown in Table 5. When the relative wind velocity measured on board is converted into true wind velocity, it is approximately 5 m/s or less. The height of wind wave and swell is less than 1.1 m. Hence, the environmental condition in sea trial is moderate.

4.2. Uncertainty analysis due to the increase in resistance of wind

The additional resistance due to wind can be calculated using Eq. (7). This equation is a function of true wind velocity, true wind direction, ship speed, and projected area of a superstructure. The coefficient of drag (C_{AA}) of wind is dependent on ship type and true wind direction. The coefficient can be estimated using the ITTC chart, wind tunnel test, and CFD analysis. In this study, ITTC chart is used to estimate the drag coefficient.

$$R_{AA} = 0.5 \cdot \rho_A \cdot C_{AA}\left(\psi_{WRef.}\right) \cdot A_{XV} \cdot V_{WRef}^2 - 0.5 \cdot \rho_A \cdot C_{AA}(0) \cdot A_{XV} \cdot V_G^2 \quad (7)$$

Table 5
Measured average wind and wave data in sea trials.

	V_{WR} (m/s)	ψ_{WR} (°)	H_W, H_S (m)	T_W,T_S (sec)	D_W, D_S (°)
50%	15.4	358	0.6, 1.0	5.5, 10.2	7, 157
	3.4	322	0.6, 1.1	5.7, 10.4	144, 324
70%	15.8	357	0.6, 0.9	5.4, 10.3	7.0, 173
	4.7	331	0.6, 0.8	5.5, 10.1	202, 333
80%	16	357	0.6, 1.0	5.4, 10.6	359, 165
	5.7	338	0.6, 0.8	5.5, 10.3	164, 333

Table 6a
Uncertainty of type-B on the wind measurement system.

Item	Uncertainty of type-B
Wind speed	10 m/s or less: Within ±0.5 m/s 10 m/s or more: Within ±5%
Wind direction	±5°

Vane anemometers are currently the most widely used instruments to measure wind speed. The most common types of anemometers used in ships are reviewed, and the accuracy of vane anemometers is listed in Table 6.

Fig. 9 shows the raw data of relative wind velocity and direction measured at MCR 70% condition. The number of total measured samples is approximately 120 for 10 min. The average values of relative wind velocity and direction are 15.8 m/s and 357°, respectively, and the difference between the maximum and minimum values of relative wind velocity and direction are 12° and 3.8 m/s, respectively.

The analysis results of goodness of fit test for relative wind direction and wind velocity exhibit Gaussian distribution, as shown in Fig. 10. Thus, the relative wind direction and wind speed measured for 10 min in the sea trial constantly deviate around the average values.

Based on the type-B uncertainty of the anemometer and type -A uncertainty of measured wind data in sea trials, Monte Carlo simulation is performed 50,000 times to estimate the uncertainty of the added resistance via Eq. (7). Table 6 summarizes the results of the uncertainty analysis of the added resistance due to wind.

The average of the added resistance due to wind in the first and second run under MCR 50% is approximately 93.5 kN and −55 kN, respectively. The expanded uncertainty for the two runs at MCR 50% in the 95% confidence interval is ±34.7% and ±22.0%, respectively. For the first and second run at MCR 70%, the expanded uncertainty of added resistance due to wind is ±22.8% and ±14.2%,

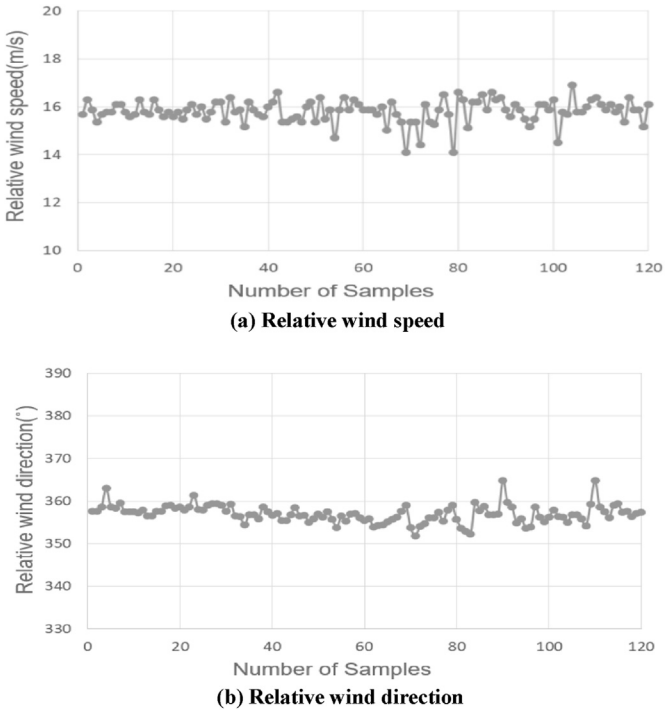

Fig. 9. Raw data of measured wind properties (MCR 70%).

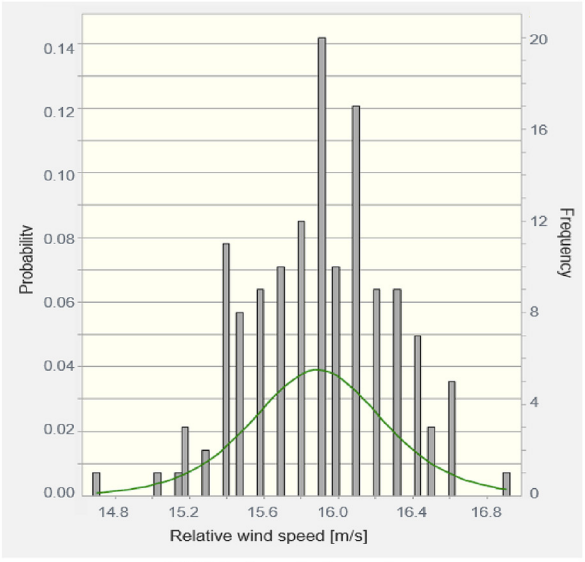

(a) Relative wind speed

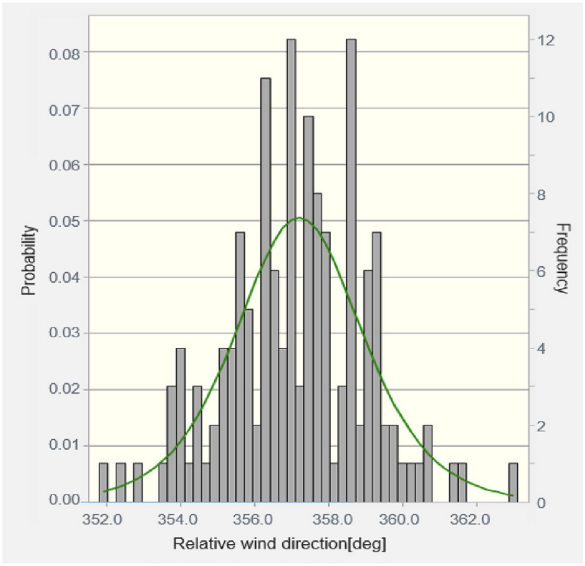

(b) Relative wind direction

Fig. 10. Probability distribution on measured wind properties (MCR 70%).

Table 6b
Results of uncertainty analysis on added resistance due to wind.

MCR	Double run	R_{AA} (kN)	U (95%, k = 2) (kN)	U (95%, k = 2) (%)
50%	1st run	93.5	±32.4	±34.7
	2nd run	−55.0	±12.1	±22.0
70%	1st run	94.3	±21.5	±22.8
	2nd run	−60.1	±8.5	±14.2
80%	1st run	90.9	±38.8	±42.7
	2nd run	−58.6	±12.8	±21.9

respectively. The average of the added resistance due to wind in the first and second run under MCR 70% is approximately 94.3 kN and −60.1 kN, respectively, and the expanded uncertainty in the 95% confidence interval is ±42.7% and 21.9%, respectively. Furthermore, the average of the added resistance due to wind in the first and second run under MCR 80% is approximately 90.9 kN and −58.6 kN, respectively.

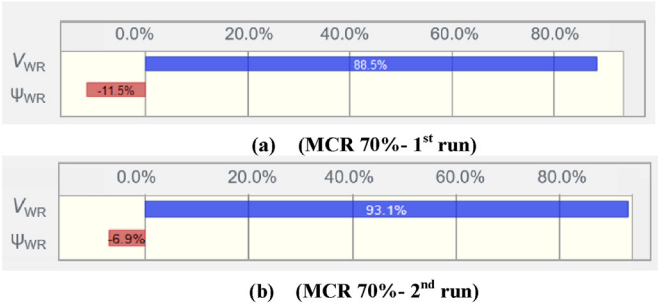

(a) (MCR 70%- 1st run)

(b) (MCR 70%- 2nd run)

Fig. 11. Contribution to variance chart of uncertainty factor on the predicted added resistance due to wind(MCR 70%).

Fig. 11 shows the results of the contribution to variance on the added resistance due to wind at MCR 70% condition. The uncertainty of added resistance due to wind is mostly affected by the relative wind velocity (V_{WR}). Hence, uncertainty in relative wind velocity contributes to the uncertainty of added resistance due to wind by 88.5% and 93.1% for runs 1 and 2, respectively. Thus, the uncertainty in the added resistance due to wind is more affected by uncertainty due to wind velocity (V_{WR}) than due to relative wind direction (ψ_{WR}). Additionally, the contribution to the relative wind direction(ψ_{WR}) was −11.5% and −6.9%, respectively. The reason marked as negative means that as the relative wind direction increases, the value of the additional resistance against the wind decreases.

4.3. Uncertainty analysis of the increase in resistance due to waves

Guidelines for the assessment of speed and power performance via analysis of speed trial data (ISO 15016, 2015) led to three methods, namely STAWAVE-1, STAWAVE-2, and a theoretical method to correct the additional resistance due to waves. Insel (2008) used a simple correction model (STAWAVE-1) to calculate the additional resistance due to waves. However, this method exhibits disadvantages that it can be used only in short wave condition because additional resistance generated by ship motion is neglected. Hence, in this study, STAWAVE-2 method is applied to consider additional resistance due to ship motion and reflected waves.

$$R_{AW} = 2\int_0^{2\pi}\int_0^{\infty} \frac{R_{wave}(\omega,\alpha,V_S)}{\xi_A^2} E(\omega,\alpha)\,d\omega\,d\alpha$$

$$R_{wave} = R_{AWML} + R_{AWRL}$$

$$R_{AWML} = 4\rho s g \xi_A^2 \frac{B^2}{L_{PP}} \bar{r}_{aw}(\omega) \tag{8}$$

$$R_{AWRL} = \frac{1}{2}\rho s g \xi_A^2 B \alpha_1(\omega)$$

R_{AW} denotes the sum of the additional resistance due to waves, which is expressed by the sum of additional resistance due to ship motion and reflected waves (Eq. (8)). The data of wave height, direction, and period are necessary to estimate the correction value of additional resistance due to waves. If there is a swell in sea trials, the data of swell height, direction, and period are also required. Given that the STAWAVE-2 method is considered only for incident waves with a direction within ±45° of bow, it is assumed that a wave direction of ±45° or more does not affect the additional resistance due to waves.

Table 7
Uncertainty of type-B on the wave measurement system.

Item	Uncertainty of type-B
Wave height	±10% or ±0.5 m
Period	±0.5 s
Direction	±5°

According to ISO 15016(2015), sea trials should be conducted in water that is calm to the maximum possible extent. This is to reduce the uncertainty of the correction due to added resistance. However, if the sea trial cannot be performed in mild sea conditions, the characteristic data of waves should be accurately measured. The characteristic data of waves can be measured via eye measurement, buoy, radar, and weather data. In this study, weather data was used for wave height, direction, and period, so uncertainty of type-B were considered to examine added resistance due to wave. The uncertainty of wave characteristics is assumed to be ±10% for wave height, ± 0.5 s for wave period, and ±5° for wave direction, as listed in Table 7.

The probability distribution of wave height is assumed as Gaussian, and the probability distribution of wave period and direction is assumed as rectangular.

Table 8 shows the results of the uncertainty analysis on added resistance due to waves. The uncertainty of the added resistance due to waves was uniformly approximately ±21% in a 95% confidence interval in all conditions.

4.4. Uncertainty of delivered power in the ideal power

The shaft torque and shaft speed should be measured to predict the ideal delivered power of a ship. Additionally, environmental conditions, such as wind velocity, wind direction, wave height, wave period, wave direction, water temperature, and water depth, should also be measured to correct for the effects of disturbances in sea trials. Hence, the estimated delivered power in ideal conditions inevitably includes various systematic and environmental uncertainty factors.

The uncertainty factors that can be included when estimating the delivered power in ideal conditions via the method in ISO 15016(2015) guideline are shown in Fig. 12. The uncertainty factors can be broadly divided into uncertainties of the shaft power measurement system and uncertainties of the correction due to environmental effects.

The total uncertainty of the measurement system for shaft power includes uncertainties in the shaft torque and shaft speed. Additionally, uncertainties due to correction for environmental effects are composed of uncertainties due to added resistance (R_{AA}) of wind, added resistance (R_{AW}) of waves, and added resistance (R_{AS}) of water temperature and density.

The shaft power measured during sea trials should be converted to that for calm water conditions such as model test conditions. Hence, it is necessary to correct the term for environmental disturbance according to ISO 15016(2015). The probability distributions of measured shaft power and total added resistance due to environmental disturbance are necessary to estimate the uncertainty of shaft power and expanded uncertainty at ideal conditions.

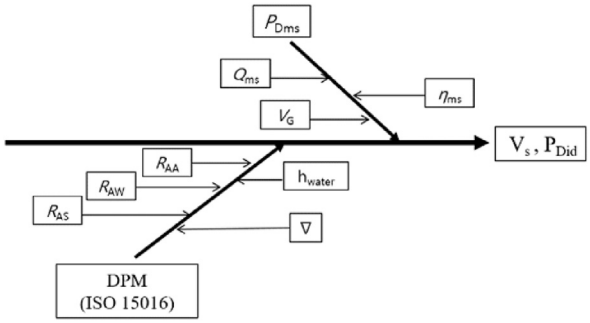

Fig. 12. Uncertainty sources in sea trial (Seo et al., 2019). P_{Dms}: delivered power in the trial condition; P_{Did}: delivered power in the ideal condition; Q_{ms}: measured torque at the propeller shaft; V_G: measured speed of ship over ground; R_{AA}: resistance increase due to wind; R_{AW}: resistance increase due to wave; R_{AS}: resistance increase due to deviation of water temperature and density; h_{water}: water depth; ∇: displacement volume.

Thus, based on the probability distribution obtained in the previous section, Monte Carlo simulation was conducted via Eq. (9).

$$P_{Did} = P_{Dms} - \left(\frac{\Delta R V_S}{\eta_{Did}} + P_{Dms}\left(1 - \frac{\eta_{Dms}}{\eta_{Did}}\right)\right) \tag{9}$$

where.

P_{Did}: delivered power in the ideal condition.
P_{Dms}: delivered power in the trial condition.
ΔR: total increase in resistance
n_{Did}: propulsive efficiency coefficient in the ideal condition.
n_{Dms}: propulsive efficiency coefficient in the trial condition.
Vs: ship speed through the water.

V_s is the ship speed through the water, but the average value of the ground speed(V_G) can be used as the ship speed through the water(V_s) when a double run test is performed in sea trial(ISO 15016, 2015). Since the ship speed over ground(V_G)is known to be quite precise because it usually uses the Difference Global Positioning System (DGPS), the uncertainty of ship speed was ignored in this study.

Table 9 shows the results of the uncertainty analysis on the shaft power corrected to ideal conditions such as calm sea at all MCR conditions. In case of MCR 50% and 80%, expanded uncertainty of shaft power at ideal conditions is approximately ±1.4% in the 95% confidence interval at a coverage factor of 2. In the MCR 70% condition, the expanded uncertainty is estimated to be as low as ±1.1% in the 95% confidence interval (k = 2). This implies that the reliability of measured and corrected delivered shaft power in ideal condition is high.

Fig. 13 shows the results of probability and frequency on delivered power in ideal condition under the MCR 70%. The average value is approximately 30,248 kW and the expanded uncertainty of ideal power is ±334 kW in the 95% confidence interval (k = 2). If the

Table 8
Uncertainty results of added resistance due to wave.

MCR	Double run	R_{AW} (kN)	U (95%, k = 2) (kN)	U (95%, k = 2) (%)
50%	1st run	8.1	±1.6	±20.3
	2nd run	41.3	±8.4	±20.3
70%	1st run	8.6	±1.7	±20.1
	2nd run	33.4	±6.9	±20.7
80%	1st run	8.6	±1.7	±20.2
	2nd run	27.7	±5.7	±20.7

Table 9
Uncertainty for corrected delivered power in the ideal condition.

MCR	U (95%, k = 2)
50%	±1.4%
70%	±1.1%
80%	±1.4%

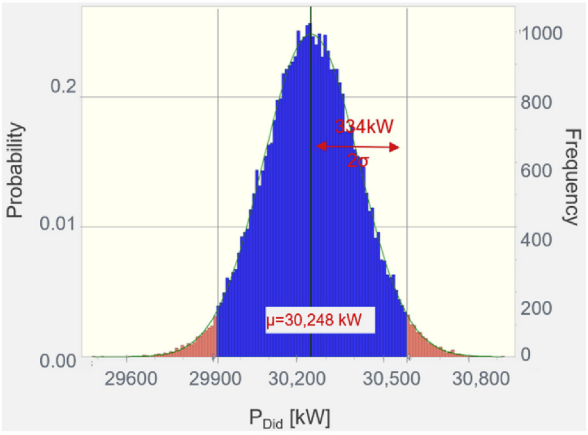

Fig. 13. Uncertainty for corrected power (MCR 70%).

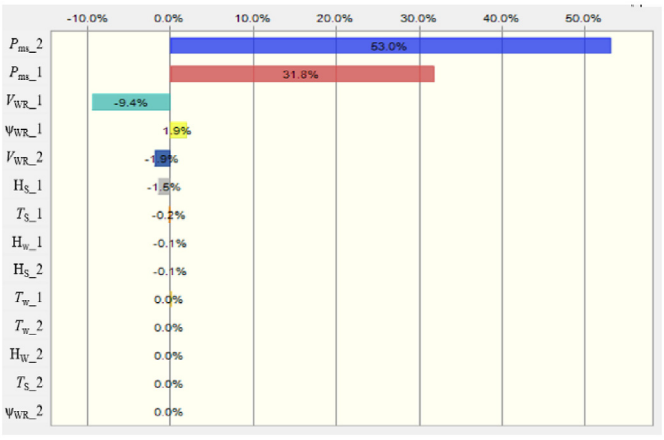

Fig. 14. Contribution to variance chart of uncertainty factor on the corrected power (MCR 70%).

estimated expanded uncertainty of delivered power in ideal condition is converted to expanded uncertainty of ship speed, it corresponds to approximately ±0.14 knots at a shaft power of 30,000 kW.

Fig. 14 shows the contribution to the distribution of the delivered power (P_{Did}) in ideal condition. The contribution is estimated with the results of the double run test at MCR 70%. The shaft power measurement system has the maximum impact at 70% MCR condition with a contribution of 32% and 53% in case of P_{ms}_1 and P_{ms}_2, respectively, during the double run test. It accounts for 85% of the total distribution. The second factor is the wind speed (V_{WR}-1), which accounts for approximately 10%. Thus, most of the uncertainties are generated by the shaft power measurement system. This because the sea trial was conducted in moderate sea conditions with extremely small corrections for the environmental disturbance, which in turn had low impact on the total delivered power. In addition, the reason that the contribution rate of some uncertainty factor is marked as negative is to simply express that there is an inverse relationship with the corrected power.

5. Conclusion

In this study, we performed uncertainty analysis of ship speed–power performance based on raw data acquired during sea trial. The speed–power performance was estimated as per the guidelines of ISO 15016(2015), and Monte Carlo simulation was used for the analysis of uncertainties.

1) The expanded uncertainty of added wind resistance was ±22.8% and ±14.2% at MCR 70% condition. Additionally, the expanded uncertainty of added wave resistance was ±20.1% and ±20.7% at a 95% confidence interval (k = 2).
2) The expanded uncertainty of the measured delivered power (P_{Did}) at the MCR 70% condition converted to the ideal conditions was approximately ±1.1% while that at MCR 50% and 70% conditions was approximately ±1.4%.
3) The uncertainty due to the shaft power measurement system was the highest component of the uncertainty factor for the delivered power in ideal condition. It accounts for approximately 60% of the total uncertainty. Hence, it is necessary to measure the shaft torque more precisely to reduce the uncertainty due to the shaft power in sea trials.
4) The sea trials considered in this study were performed in relatively moderate sea water, and thus the component of the added resistance due to disturbance to the total ship resistance was not high. Thus, it was concluded that the influence of the added resistance on the uncertainty of ship speed–power performance during the sea trial was minor, and thus the shaft power measurement system exhibited a dominating effect.

In order to generalize the uncertainty analysis results, uncertainty analysis will be performed based on the raw data of sea trials various ship in the future.

Declaration of competing interest

The authors declare that they have no known competing financial interests or personal relationships that could have appeared to influence the work reported in this paper.

Acknowledgements

This paper was supported by research funds of Kunsan National University and Ministry of Oceans and Fisheries (No. 20210631(KIMST), Development of Smart Port-Autonomous Ships Linkage Technology), Korea.

References

Aldous, L.G., 2015. Ship Operational Efficiency: Performance Models and Uncertainty Analysis. Doctoral Thesis. University College, London, United Kingdom.
Brown, A., Chen, D., 2002. Probabilistic method for predicting ship collision damage. Ocean Engineering International Journal 6, 55–65.
Coleman, H.W., Steele, W.G., 2009. Experimentation, Validation, and Uncertainty Analysis for Engineers, third ed. John Wiley & Sons, Inc.
Coraddu, A., Figari, M., Savio, S., 2014. Numerical investigation on ship energy efficiency by Monte Carlo simulation. Journal of Engineering for the Maritime Environment 228, 220–234.
Han, B.W., Seo, J.H., Lee, S.J., et al., 2017. Uncertainty assessment for a towed underwater stereo PIV system by uniform flow measurement. International Journal of Naval Architecture and Ocean Engineering 10, 596–608.
Hang, H.Y., Xiao, L., Yang, M.X., 2018. Hull lines reliability-based optimisation design for minimum EEDI. Journal Brodogradnja 69, 17–33.
Insel, M., 2008. Uncertainty in the analysis of speed and powering trials. Ocean. Eng. 35, 1183–1193.
International Towing Tank Conference (ITTC), 2002. Final Report and Recommendations to the 23rd ITTC - the Specialist Committee on Speed and Powering Trials.
International Towing Tank Conference (ITTC), 2005. Recommended Procedures and Guidelines – Testing and Extrapolation Methods Loads and Responses, Seakeeping Experiments (7.5-02-07-02.1).
ISO 15016, 2015. Ships and Marine Technology — Guidelines for the Assessment of Speed and Power Performance by Analysis of Speed Trial Data.
ISO 19030, 2016. Ships and Marine Technology – Measurement of Changes in Hull and Propeller Performance.
ISO JCGM 100, 2008. Evaluation of Measurement Data - Guide to the Expression of

Uncertainty in Measurement.
ISO JCGM 101, 2008. Evaluation of Measurement Data – Guide to the Expression of Uncertainty in Measurement- Propagation of Distributions Using Monte Carlo Method.
Kinaci, O.K., Gokce, M.K., Alkan, A.D., et al., 2018. On self-propulsion assessment of marine vehicles. Journal Brodogradnja 69, 29–51.
Liang, Qingxue, Hu, Hao, 2017. Uncertainty analysis of value for money assessment for public-private partnership projects. Journal of Shanghai Jiatong University 22 (6), 672–681.
Park, D.W., Kim, M.G., Kang, S.H., 2003. Uncertainty analysis for the resistance and self-propulsion test of ship model. Journal of the Society of Naval Architects of Korea 40, 1–9.
Park, D.M., Lee, J.H., Kim, Y., 2015. Uncertainty analysis for added resistance experiment of KVLCC2 ship. Ocean. Eng. 94, 143–156.
Park, D.M., Kim, T.Y., Kim, Y., 2012. Study on numerical sensitivity and uncertainty in the analysis of parametric roll. Journal of the Society of Naval Architects of Korea 49, 60–67.
Para-Gonzalez, L., Mascaraque-Ramires, C., Madrid, E., 2018. Obtaining the budget contingency reserve through the Monte Carlo method: study of a ferry construction project. Journal Brodogradnja 69, 79–95.
Seo, S., Song, S., Park, S., 2016. A study on CFD uncertainty analysis and its application to ship resistance performance using open source libraries. Journal of the Society of Naval Architects of Korea 53, 329–335.
Seo, D.W., Kim, M.S., Kim, S.Y., 2019. Uncertainty analysis for speed and power performance in sea trial using Monte Carlo simulation. Journal of the Society of Naval Architects of Korea 56 (3), 242–250.
Sun, L., Zhang, Q., Ma, G., et al., 2017. Analysis of ship collision damage by combining Monte Carlo simulation and the artificial neural network approach. Journal Ships and Offshore Structures 12, S21–S30.
Tillig, F., Ringsberg, J., Mao, W., Ramne, B., 2018. Analysis of uncertainties in the prediction of ships' fuel consumption – from early design to operation conditions. Journal Ships and Offshore Structures 13, S13–S24.